Modeling and Simulation of Grid Inverter in Grid-Connected Photovoltaic System

Atiqah Hamizah Mohd Nordin*‡, Ahmad Maliki Omar**, Hedzlin Zainuddin***

*Faculty of Electrical Engineering, Universiti Teknologi MARA, Pasir Gudang, Johor, Malaysia
**Faculty of Electrical Engineering, Universiti Teknologi MARA, Shah Alam, Malaysia
***Faculty of Applied Science, Universiti Teknologi MARA, Shah Alam, Malaysia
atiqah.hamizah@gmail.com, ambomaliki@gmail.com, hedzlinzainuddin@yahoo.com

‡Corresponding Author: Atiqah Hamizah Mohd Nordin; Universiti Teknologi MARA, Pasir Gudang, Johor, Tel: +60 73818195, atiqah.hamizah@gmail.com

Received: 11.09.2014 Accepted: 07.11.2014

Abstract- This paper presents the development of inverter simulation model in Grid-Connected Photovoltaic System (GCPV) in Matlab/Simulink software. This work is a part of the development of a complete GCPV system simulation model. The inverter simulation model accepts solar irradiance and temperature parameters as inputs (at PV array) and outputs AC power. A phase-shift control method is used to ensure that the inverter output is synchronized with unity power factor to the utility grid. The developed model is validated against data obtained from an actual installed GCPV system at Malaysia Green Technology Corporation (MGTC) in Bangi, Malaysia with system capacity of 45.35 kWp. The validation of model is through Root Mean Square Error (RMSE) and Mean Absolute Percentage Error (MAPE). Results showed that inverter output power from simulation is acceptable with small deviation from the actual data. This is due to inaccuracies of predicting de-rating factors listed in this work.

Keywords—Photovoltaic; solar; grid inverter; simulation; de-rating factor.

1. Introduction

In grid-connected photovoltaic system (GCPV), the grid inverter is crucial to convert the DC power which is generated from the photovoltaic (PV) arrays into the AC power to match with the grid voltage and frequency. Basically, a typical GCPV system consists of PV array, maximum power point tracker (MPPT) unit(s), inverter and utility grid and can be represented in the block diagram as depicted in Fig. 1.

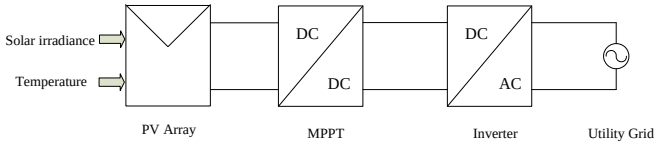

Fig.1. A typical GCPV system block diagram

PV array convert sunlight energy into DC electricity. In practice, PV array is connected to a maximum power point tracker (MPPT) in order to allow the PV array to produce maximum power it is capable of. The produced DC power is then converted into AC power using inverter before delivered into the utility grid. Usually, the MPPT is built-in in the inverter.

The grid inverter is different from a typical inverter that used in stand-alone PV system. The main specification of the grid inverter is that current drawn from the inverter is delivered to the utility grid at unity power factor. Recently there are inverters that having adjustable power factor. There are several grid inverter technologies for PV applications available such as centralized inverter, string inverter, multi-string inverter and modular inverter [1-3].

Various studies on modeling PV system components show that it has become increasingly important in the PV system development. By modeling PV system using simulation software, the system could be evaluated and analyzed without adjusting the real system and this is major saving in cost and time.

This work will focus on the inverter modeling, which is a part of the development of a complete GCPV system

simulation model [4]. The developed model is validated by comparing the simulation output with the data obtained from an installed GCPV system at Malaysia Green Technology Corporation (MGTC) in Bangi, Malaysia. The installed GCPV system which is also known as Pack A1 system has an installed capacity of 45.35 kWp.

2. Methodology

2.1 Inverter Desgin

The centralized inverter topology is applied at the Pack A1 PV system at MGTC. The centralized inverter topology at the Pack A1 PV system consists of three units of single-phase inverter. This study however will concentrate only on one of the single-phase inverter units. Therefore the output power of the inverter from the simulation will be converted into the equivalent three-phase value, to compare with the actual values from the actual data which is available in three-phase values.

The inverter model in this study is designed by referring to the specification of the Pack A1 system's inverter which is Fronius IG500 as listed in Table 1.

Table 1. Specification of Fronius IG500 Inverter

	Subjects	Descriptions
Input data	Recommended power supply	40 – 52 kWp
	MPP voltage range	210 – 420 V
	Maximum input voltage	530 V
	Maximum input current	205 A
Output data	Nominal output power	40 kW
	Nominal frequency	50 ± 0.2 Hz
	Distortion factor	< 5 %
	Power factor	1
General data	Maximum efficiency	94.3 %

A single-phase full-bridge inverter is modeled in this study. The semiconductor switches used is IGBT as it can handle very large power, which is suitable for this PV system. Fig. 2 shows the schematic diagram of the developed grid inverter model in GCPV system. Using bipolar switching scheme, the full-bridge inverter has two switching states as outlined in Table 2. The PWM inverter output waveform is then filtered to produce a sinusoidal AC waveform.

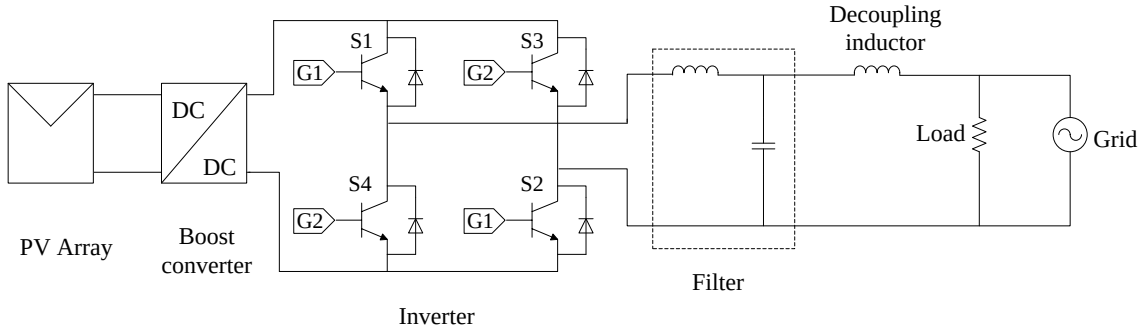

Fig. 2. Inverter schematic diagram in GCPV system

Table 2. Switching States of Single-Phase Full-Bridge Inverter

Switching state	Switches ON	Switches OFF	Pulse output voltage
1	S1, S2	S3, S4	+Vdc
2	S3, S4	S1, S2	-Vdc

The inverter switching is controlled by the sinusoidal PWM (SPWM) gating signals which drive the gate of the IGBTs. In order to generate the gating signal (V_g) for the IGBTs by implementing the bipolar switching scheme, there are two inputs for the comparator which are a sinusoidal modulating signal (V_m) and a triangular carrier signal (V_{cr}). When V_m has higher magnitude than V_{cr}, the comparator output is high (ON), otherwise it is low (OFF). The gating signal generation which is illustrated in term of waveform is depicted in Fig. 3.

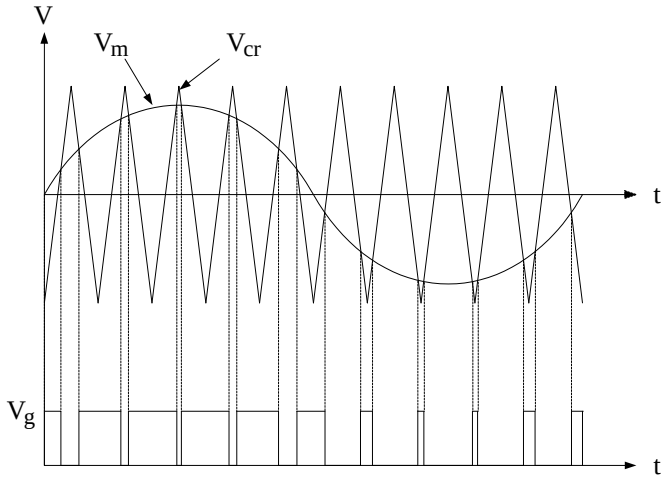

Fig. 3. V_g generation

The output voltage of the inverter is controlled by the amplitude, phase and frequency of V_m. The amplitude of V_m (A_m) controls the modulation index, M as in Eq. (1), thus controls the amplitude of inverter output voltage.

$$M = \frac{A_m}{A_{cr}} \quad (1)$$

Where,

M = modulation index (decimal)

A_m = amplitude of modulating signal (V)

A_{cr} = amplitude of carrier signal (V)

The phase angle of V_m influences the phase of the inverter output voltage. The appropriate value of phase angle of V_m should be selected in order to match the grid current phase to obtain the unity power factor. The frequency of V_m will determine the frequency of the inverter output voltage. The switching frequency (f_s) of the inverter depends on the frequency of V_{cr}. In the developed model, the modulating signal frequency (f_m) is set to 50 Hz to match the frequency of the utility grid, while fs is set to 10 kHz.

In reality, switching frequency of 20 kHz or above is commonly used to operate outside the audible noise. Generally, the level of audible noise decreases with the increase of switching frequency [5]. However in simulation, a very high switching frequency (20 kHz or above) will require a very small value of simulation step size (μs or less) for accurate switching simulation studies which will result in very long simulation time [6]. The simulation step size used in this simulation studies is 1 μs.

2.2 Low-pass LC Filter Design

The SPWM waveform of the inverter output voltage contains harmonics. According to the IEC 61727 standard (PV System, characteristics of the utility interface), the maximum allowed THD for the output current is 5 % . Therefore an LC filter is a crucial part in designing the grid inverter. The LC filter is needed to filter out undesired switching frequency components from the inverter output current spectrum. The LC filter which is connected to the output of the inverter circuit should be able to generate a sinusoidal output current with THD less than 5 %.

The low-pass LC filter is designed accordingly so that the cut-off frequency, f_c is higher than the grid frequency and lower than the inverter switching frequency, based on Eq. (2). The chosen f_c for the model is 1 kHz. Therefore the inductance and capacitance values of 10 mH and 2.53 μF are chosen for the LC filter.

$$f_c = \frac{1}{2\pi\sqrt{L_f C_f}} \quad (2)$$

Where,

f_c = cut-off frequency (Hz)

L_f = filter inductor (H)

C_f = filter capacitor (F)

2.3 Grid Synchronization

Grid inverter needs a pure sinusoidal reference voltage to ensure that the sinusoidal output of the inverter is synchronized to the grid frequency. The voltage magnitude of the inverter output (V_{inv}) needs to exceed the grid voltage, (V_{grid}) to enable the inverter current (I_{inv}) to be supplied to the grid. Fig. 4 shows the V_{grid}, V_{inv}, I_{inv} and voltage across decoupling inductor (V_{XL}) in the equivalent circuit at the AC side of the inverter. The decoupling inductor, XL is

needed to control the power flow from the inverter to the grid.

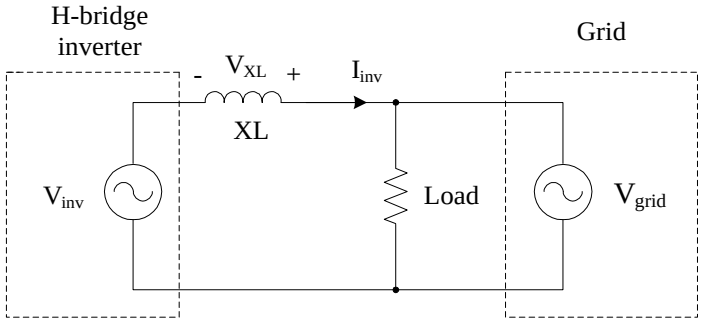

Fig. 4. Equivalent circuit at AC side of the inverter

In order to achieve the unity power factor, the waveform of Iinv must be in phase with the waveform of V_{grid} as illustrated in Fig. 5. In the phasor diagram, it is represented as in Fig. 6. As in Fig. 6, V_{inv} has to lead V_{grid} with the angle α in order to get the I_{inv} in phase with the V_{grid}. This is achieved by adjusting the phase angle of the modulating signal (V_m).

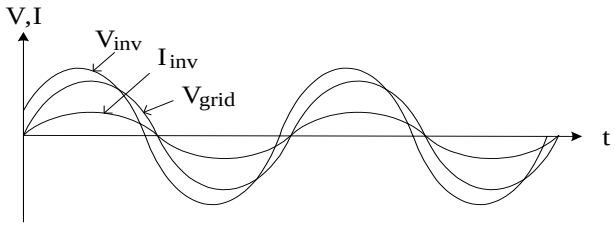

Fig. 5. Waveforms of V_{inv}, I_{inv} and V_{grid}

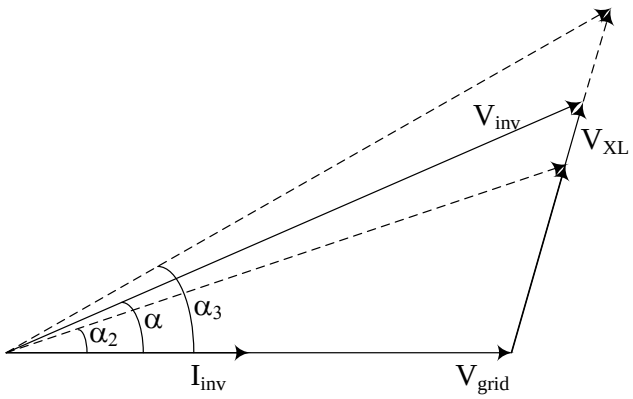

Figure 6. V_{inv}, I_{grid} and V_{grid} in phasor diagram

The phase angle of modulating signal (V_m) is varied with solar irradiance and temperature level in order to get the I_{inv} synchronized with the V_{grid}. The appropriate phase angle for a certain range of temperature and irradiance level has to be set. In the developed model, the phase angle of V_m will automatically change to the appropriate value according to the range of cell temperature level. For simplicity, since there is a quite linear relationship between solar irradiance and cell temperature, the developed model will only detect the solar irradiance value for controlling the selection criteria of phase angle value.

2.4 Simulation Work

The inverter is modeled in circuit-based approach as shown in Fig. 7. The 'inverter switching' subsystem in Fig. 7 contains the switching signal generation for the IGBTs and also the subsystem of the grid synchronisation control as depicted in Fig. 8. The repeating sequence block is set to generate triangular carrier signal (V_{cr}) with the frequency of 10 kHz. The sinusoidal modulating signal (V_m) is generated using the sinusoidal AC voltage source block with the frequency of 50 Hz. The relational operator is used as the comparator to compare V_{cr} and V_m to produce the V_g. The 'NOT logical operator' block is used to invert the V_g signal for the inverter switching.

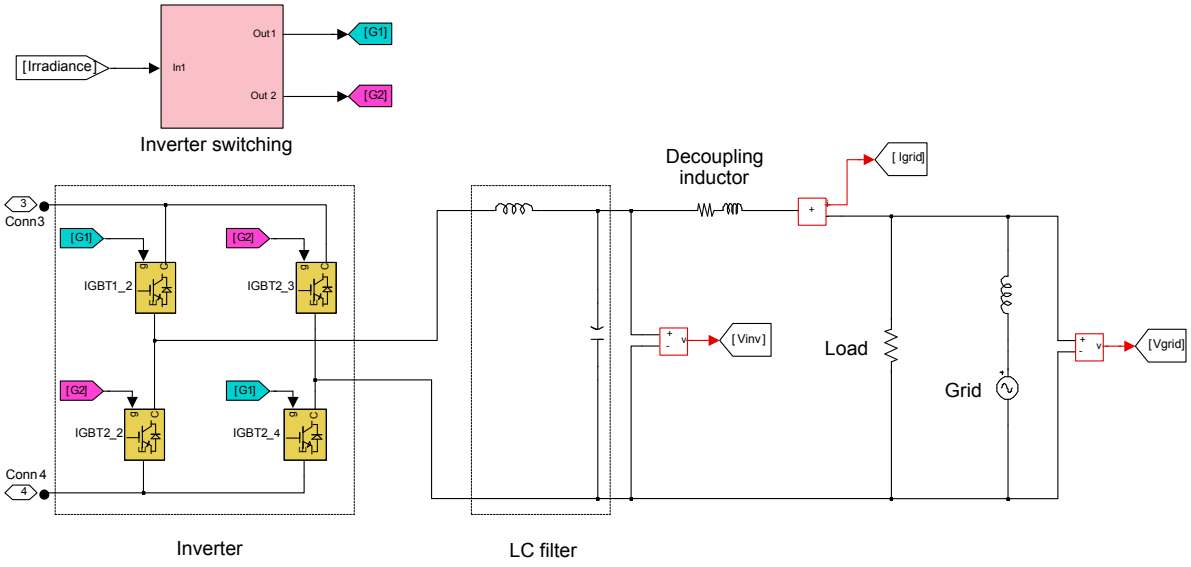

Fig. 7. Inverter, LC filter and utility grid circuit

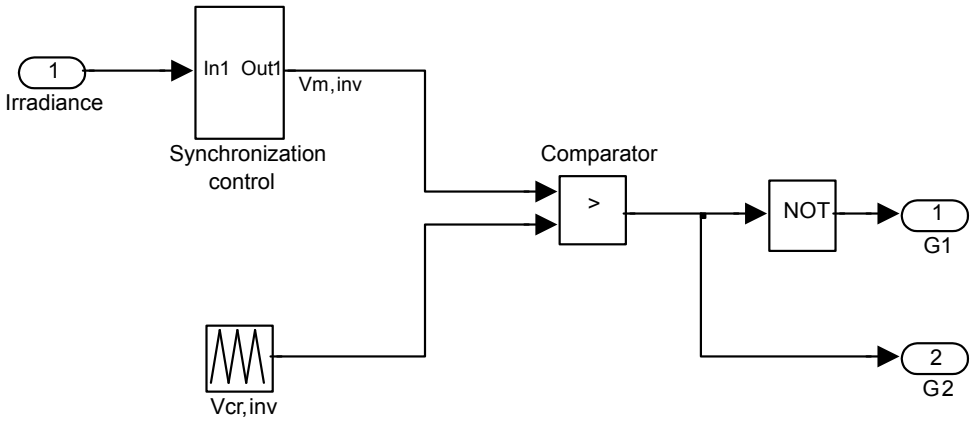

Fig. 8. Inverter switching signal generation

Note that the synchronization control subsystem in Fig. 8 comprises of several sinusoidal AC voltage source blocks with different phase values. A switch is used to select the AC voltage source block with the appropriate phase value in order to synchronize to the grid. The selection of the source phase is according to the solar irradiance input of the system using lookup table approach.

The low-pass LC filter is connected to the output of the inverter. The decoupling inductor with inductance value of 2 mH is connected in series with the LC filter. A resistor which acts as the load with value of 5 Ω is connected in parallel to the decoupling inductor as shown in Fig. 7. The grid is modeled using an AC voltage source block while an inductor with value of 1 mH which is connected in series to the grid acts as transmission line. Terminal 3 and 4 in the circuit in Fig. 7 are the connection from the boost converter developed in [4].

3. Results and Discussion

3.1 Without Consideration of De-rating Factors

First, consider ideal case condition. Fig. 9 shows the measurement positions of the V_{inv}, V_{grid} and I_{inv}. The V_{inv} is measured at the output terminal of the LC filter. The I_{inv} is measured in series with the decoupling inductor, and the V_{grid} is measured across the grid source and the inductor which act as the transmission line.

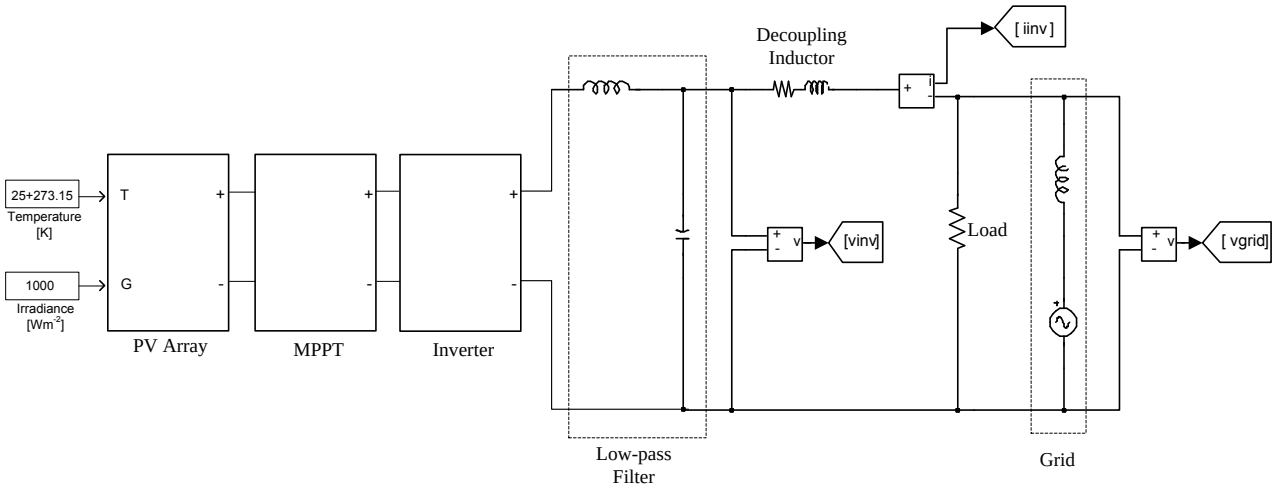

Fig. 9. Measurement positions of I_{inv}, V_{inv} and V_{grid}

Fig. 10 shows the sinusoidal waveforms of the V_{grid} and I_{inv} of the simulated model for the solar irradiance of 808 Wm^{-2} and temperature of 69.51°C. It is observed that the I_{inv} waveform is in phase with the V_{grid} waveform, which means that the inverter has synchronized to the grid. Fig. 11 shows the frequency spectrum of I_{inv} until 40th order of harmonics, at G = 808 Wm^{-2} and T = 69.51 °C which is obtained from Fast Fourier Transfer Analysis tool in Matlab Simulink software. It shows that the THD of the I_{inv} at T = 69.51 °C and G = 808 Wm^{-2} is found to be 0.51 %. The THD of the I_{inv} for several levels of solar irradiance input are also listed in Table 3. It is observed that the THD values of I_{inv} from the simulation for varying solar irradiance level are less than the maximum THD allowed according to the IEC 61727 standard which is 5 % [7].

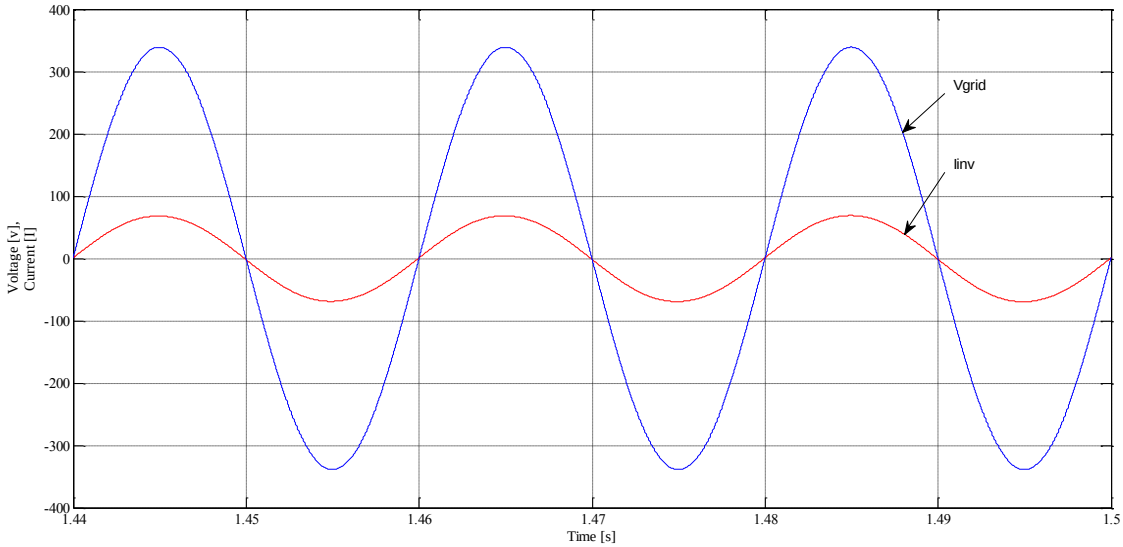

Fig. 10. Waveforms of I_{inv} synchronized to V_{grid}

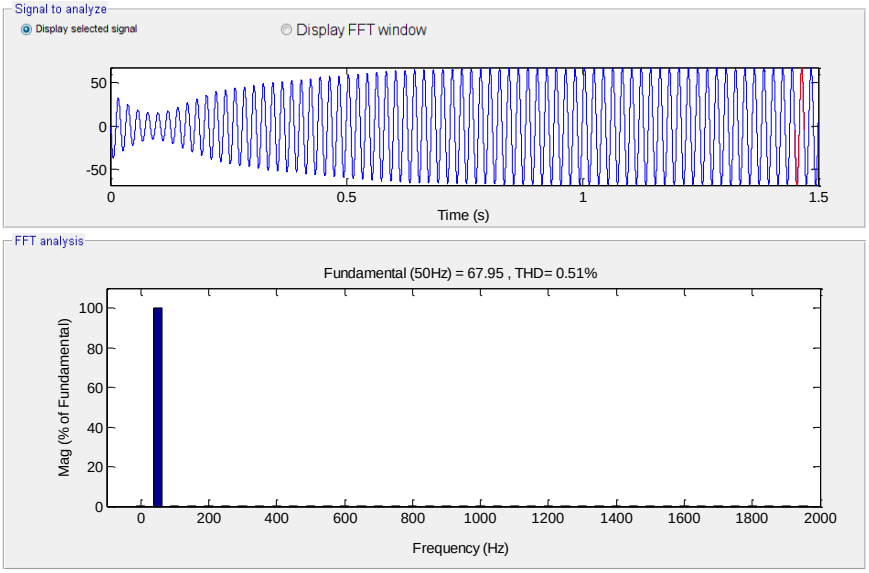

Fig. 11. THD of I_{inv} at G=808 Wm^{-2} and T=69.61°C

Table 3. THD of Iinv for varying solar irradiance level

Irradiance (Wm^{-2})	THD of I_{inv} (%)
928	0.56
808	0.51
747	0.55
666	0.48
582	0.43

The AC power produced is defined as the product of I_{inv} and V_{grid} as in Eq. (3) as given below.

$$P_{ac} = I_{inv} \times V_{grid} \times cos\ \emptyset \quad (3)$$

Where,

P_{ac} = AC power (W),

I_{inv} = inverter output current (A),

V_{grid} = grid voltage (V),

$\emptyset$ = displacement angle (degree).

The output AC power of the simulation model and the actual data for the varying solar irradiance is plotted in Fig. 12. Fig. 12 also shows the comparison between the simulated and actual AC power. Note that the output AC power value of the simulation model is already converted into three phase power by multiplying by three so that it can be compared to the actual power value from data which is provided in three-phase. From Fig. 12, it is observed that the AC power from the simulation (P_{ac_sim}) is higher than the actual (P_{ac_actual}).

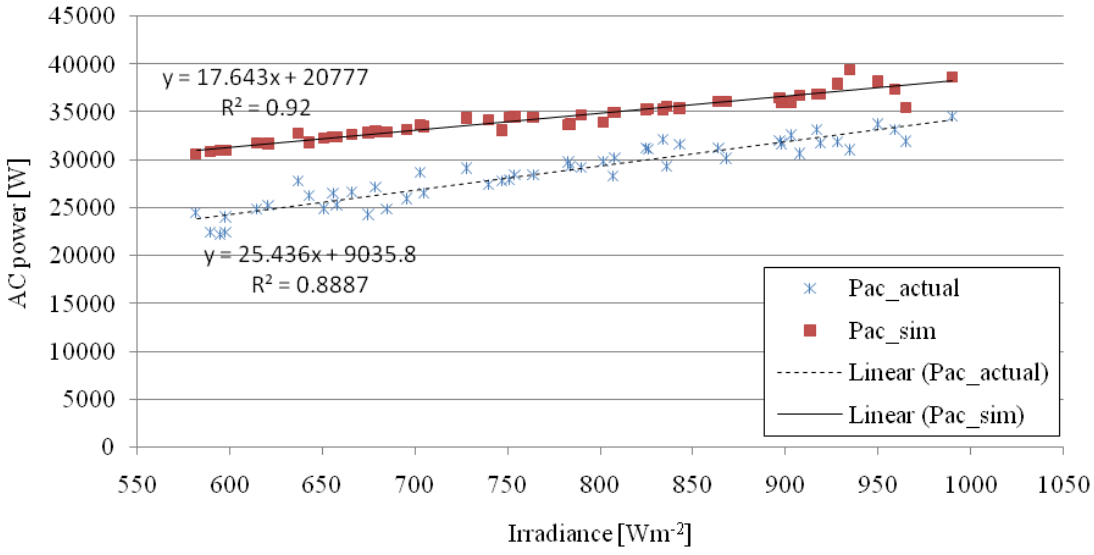

Fig. 12. AC output power against solar irradiance

The error between the simulated output and actual output is determined using the Root Mean Square Error

(RMSE) and Mean Absolute Percentage Error (MAPE). The RMSE is frequently used to measure the difference between the values simulated from the model and the actual values obtained from the real system that is being modeled and is defined in Eq. (4). The calculated RMSE value has unit in Watt (W). MAPE is a measure of accuracy in a fitted-time series value and usually is expressed as a percentage. In MAPE, the absolute values of all percentage errors are summed up and the average is computed as represented in Eq. (5). MAPE is also often useful for purposes of reporting, because it is expressed in generic percentage terms that will be understandable to a wide range of users. The RMSE of P_{ac_sim} prior to P_{ac_actual} is found to be 5920.646 W and the MAPE is 20.744 %.

$$RMSE = \sqrt{\frac{\sum_{i=1}^{n}(P_{actual\_i} - P_{sim\_i})^2}{n}} \quad (4)$$

Where,

P_{actual_i} = actual power,

P_{sim_i} = simulated power,

n = number of samples.

$$MAPE = \frac{1}{n}\sum_{i=1}^{n}\left|\frac{P_{data\_i} - P_{sim\_i}}{P_{data\_i}}\right| \quad (5)$$

Where,

P_{actual_i} = actual power,

P_{sim_i} = simulated power,

n = number of samples.

3.2 With Consideration of De-rating Factors

In reality, it is important to note that in the actual grid-connected PV system, not all power generated from the PV array could be transferred into the grid. There are power losses that occur in the PV system due to some de-rating factors such as manufacturer's tolerances and module mismatch losses (f_{mm}), losses in cables (f_{cable}), dirt on the surface of PV module (f_{dirt}) and inverter efficiency (η_{inv}). Table IV summarized the value of η_{inv}, f_{mm}, f_{dirt}, and f_{cable} which are used in the simulation of the developed model. The values of f_{mm} and η_{inv} can be obtained from the PV module and inverter datasheets. The values of f_{dirt} and f_{cable} are assumed based on Malaysia's climate, frequency of rainfall, and has been used by several researchers [8].

Table 4. De-rating factors

De-rating factors	Values
$\eta_{inv,}$	0.943
f_{dirt}	0.970
f_{cable}	0.980
f_{mm}	0.950

The simulation output power need to be multiplied by f_{mm}, f_{dirt}, f_{cable} and also η_{inv} as in Table 4. In reality, some of those parameters are difficult to estimate accurately such as dirt factor, module mismatch and cable loss. The graph in Fig. 13 shows the comparison between the values of the simulation result with consideration of the de-rating factors ($P_{ac\_sim\_derate}$) and the actual values from the data (P_{ac_actual}), for varying solar irradiance. It is observed that with the consideration of the de-rating factors, $P_{ac\_sim\_derate}$ is approaching to P_{ac_actual}. The RMSE between $P_{ac\_sim\_derate}$ and P_{ac_actual} is 1790.783 W and the MAPE is 5.480 %. It is observed that the RMSE and MAPE are reduced after taking into accounts the de-rating factors.

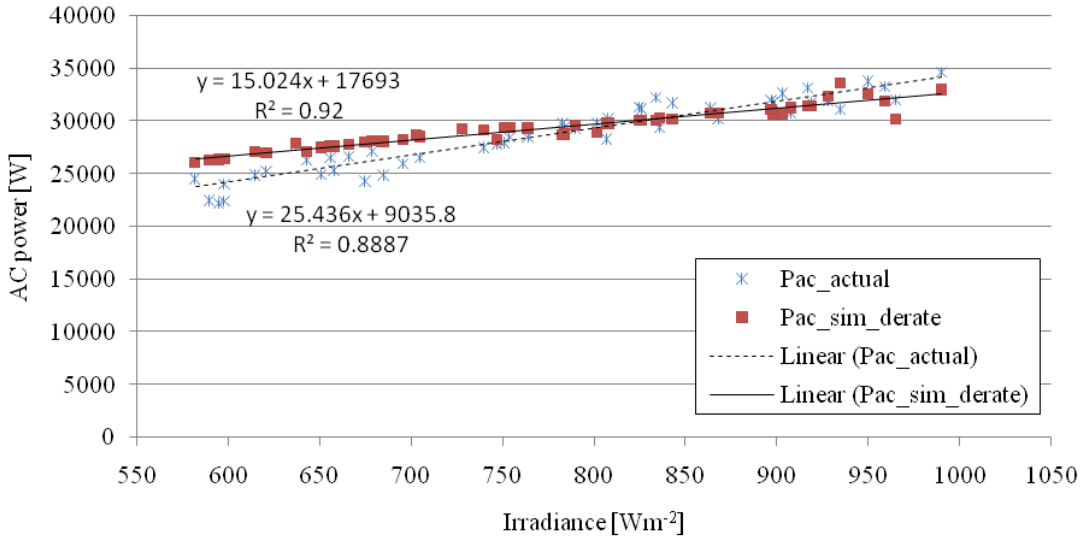

Fig. 13. AC output power with consideration of de-rating factors against solar irradiance

4. Conclusion

The single-phase full-bridge inverter for grid-connected PV power system has been developed and demonstrated. The THD of the inverter output current I_{inv} for varying solar irradiance input is below the maximum THD allowed based on the IEC 61727 standard which is 5

%. The inverter output power is also compared to the AC power obtained from the actual data using RMSE and MAPE. It is also found that the inverter output current and the grid voltage is synchronized. The consideration of f_{mm}, f_{dirt}, f_{cable} and η_{inv} at the simulation output is also important in order to get more accurate results. The RMSE and MAPE for both DC and AC sides are decreased with the consideration of these de-rating factors.

The circuit-based nature of the developed model is beneficial because it facilitates understanding of the grid-connected PV system devices and the electrical behaviour in the connected circuit and it also could be used in simulation studies of power electronic. The developed model could be improved by improving the synchronization control. The selection of phase angle of V_m has to depend on both solar irradiance and temperature value to get more accurate output power value.

Referencence

[1] S. Shaari, A. M. Omar, A. H. Haris, and S. I. Sulaiman, Solar Photovoltaic Power: Fundamentals: Ministry of Energy, Green Technology and Water, Malaysia/Malaysia Building Integrated Photovoltaic Project, 2010.

[2] S. B. Kjaer, J. K. Pedersen, and F. Blaabjerg, "A review of single-phase grid-connected inverters for photovoltaic modules," Industry Applications, IEEE Transactions on, vol. 41, pp. 1292-1306, 2005.

[3] M. Calais, J. Myrzik, T. Spooner, and V. G. Agelidis, "Inverters for single-phase grid connected photovoltaic systems-an overview," in Power Electronics Specialists Conference, 2002. pesc 02. 2002 IEEE 33rd Annual, 2002, pp. 1995-2000.

[4] A. H. M. Nordin and A. M. Omar, "Modeling and simulation of Photovoltaic (PV) array and maximum power point tracker (MPPT) for grid-connected PV system," in Sustainable Energy & Environment (ISESEE), 2011 3rd International Symposium & Exhibition in, pp. 114-119.

[5] A. Malfait, R. Reekmans, and R. Belmans, "Audible noise and losses in variable speed induction motor drives with IGBT inverters-influence of the squirrel cage design and the switching frequency," in Industry Applications Society Annual Meeting, 1994., Conference Record of the 1994 IEEE, 1994, pp. 693-700 vol.1.

[6] M. H. Nehrir and C. Wang, Modeling and control of fuel cells: distributed generated applications: John Wiley & Sons, 2009.

[7] "Photovoltaic (PV) systems - Characteristics of the utility interface," in IEC 61727, 2004.

[8] S. Shaari, A. M. Omar, A. H. Haris, and S. I. Sulaiman, Solar photovoltaic power: testing, commisioning and acceptance test of grid-connected systems: Ministry of energy, green technology and water Malaysia / MBIPV project, 2010.